Proceedings of the 9th U.S. National and 10th Canadian Conference on Earthquake Engineering
Compte Rendu de la 9ième Conférence Nationale Américaine et
10ième Conférence Canadienne de Génie Parasismique
July 25-29, 2010, Toronto, Ontario, Canada • Paper No 1565

SEISMIC DESIGN AND PERFORMANCE OF STEEL MRFs WITH ELASTOMERIC DAMPERS

Theodore L. Karavasilis[1], Richard Sause[2] and James M. Ricles[2]

ABSTRACT

This paper evaluates the hysteretic behavior of an innovative compressed elastomer structural damper and its applicability to seismic resistant design of steel MRFs. The damper is constructed by pre-compressing a high damping elastomeric material into steel tubes. This innovative construction results in viscous-like damping under small deformations and friction-like damping under large deformations. A hysteretic model for the damper is presented and calibrated using test data obtained under sinusoidal loading. A simplified design procedure is used to design seven different systems of steel MRFs combined with compressed elastomer dampers in which the properties of the MRFs and dampers were varied. The combined systems are designed to achieve performance which is similar to or better than the performance of conventional steel MRFs designed according to current seismic codes. Based on the results of nonlinear time history analyses, target properties for a new generation of compressed elastomer dampers are defined.

Introduction

Initially, passive damping systems were added to improve the seismic performance of buildings which already satisfy the strength and drift requirements of seismic codes, with the goal of reducing earthquake damage. The 2000 NEHRP recommended provisions [BSSC 2001] however, allow seismic design of buildings with passive damping systems which meet, but do not necessarily exceed the expected performance of buildings with conventional lateral force resisting systems.

This paper evaluates the hysteretic behavior of an innovative compressed elastomer structural damper [Sweeney and Michael 2006] and its applicability to seismic resistant design of steel MRFs. The damper is constructed by pre-compressing a high damping elastomeric material into steel tubes. This innovative construction results in viscous-like damping under small deformations and friction-like damping under large deformations. A hysteretic model for the damper is presented and calibrated using test data obtained under sinusoidal loading. A simplified design procedure was used to design seven different systems of steel MRFs combined with compressed elastomer dampers in which the properties of the MRFs and dampers were varied. The combined systems are designed to achieve performance which is similar to or better than the performance of conventional steel MRFs designed according to current seismic codes. Based on the results of nonlinear time history analyses to assess seismic response, target properties for a new generation of compressed elastomer dampers are defined.

[1]Dept. Lecturer, Department of Engineering Science, University of Oxford, Oxford OX1-3PJ, U.K.
[2]Professor of Structural Engineering, ATLSS Center, Lehigh University, Bethlehem, PA 18015

Compressed Elastomer Damper

Prototypes of the compressed elastomer structural damper were fabricated by bonding four pieces of an elastomer (butyl rubber blend) onto a longitudinal steel bar (Fig. 1(a)). The bar with the pieces of elastomer were then pre-compressed together into a steel tube (Fig. 1(b)). Each prototype damper included three such tubes which were welded together (Fig. 1(c)). To enable the damper to be attached to the structure, transverse bars with bolt holes were welded across the steel tubes and additional transverse attachment bars are welded across the narrow dimension of the longitudinal bars (Fig. 1(c)).

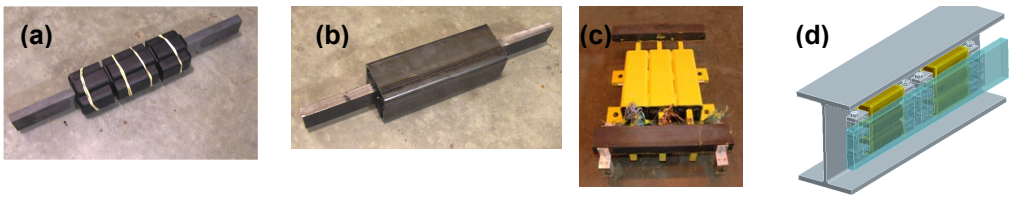

Figure 1. Fabrication of compressed elastomer damper: (a) elastomeric material wrapped around longitudinal bar; (b) elastomeric material and bar compressed into the steel tube; (c) damper with additional transverse attachment bars in place, and (d) installation to beam web

The pre-compression of the elastomer into the tube improves the performance of the bond interface between the elastomer and the longitudinal bar. The interface between the elastomer and the steel tube is not bonded, which allows the elastomer to slip relative to the tube, producing friction, when large deformations are imposed. The dampers are designed to slip before the elastomer tears or the bond to the longitudinal bar fails.

Characterization tests of the prototype damper were conducted using the NEES RTMD facility located at Lehigh University. The test setup for the tests is shown in Fig. 2. In this setup, one frame provides a reaction to the damper assembly and another frame provides a reaction to the actuator. A thick actuator clevis plate connects the actuator to the damper assembly, while a column section (loading stub) and roller bearings placed under the actuator piston assembly support the weight of the actuator and damper assembly. Each damper assembly includes two prototype dampers acting in parallel, to provide symmetry.

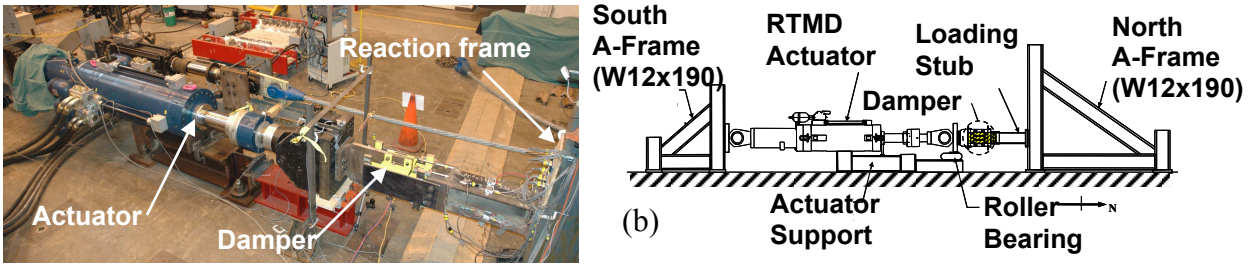

Figure 2. Compressed elastomer dampers in test setup

Characterization tests were performed on the damper which used “ramped” sinusoidal displacement histories consisting of ten complete cycles imposed on the dampers. Preliminary tests showed that the elastomer starts to slip in the tubes at a deformation amplitude of approximately 15 mm, while severe damage (debonding of the elastomer from the surface of the longitudinal bar) occurs at a deformation amplitude of approximately 45 mm. Table 1 sumarizes the various loading conditions used in the damper characterization tests.

Table 1. Loading condition parameters for characterization tests

Variables	Without slip	With slip
Deformation (mm)	3, 6, 9, 12, 15	21, 27, 33, 39, 45
Frequency (Hz)	0.5, 1.0, 1.5, 2.0, 3.0	0.5, 1.0, 1.5, 2.0, 3.0
Temperature (C^0)	15-18	15-18

Typical damper force versus damper deformation hysteresis loops are shown in Fig. 3. The damper hysteresis for the elastic (without slip) tests is viscoelastic with fairly rounded peaks (Fig. 3(a)), while the hysteresis for the tests with slip is viscoplastic (Fig. 3(b)). Note that the force shown in Fig. 3 is the total force from the damper assembly, which is composed of a pair of prototype dampers, where each damper includes three tubes as shown in Fig. 1.

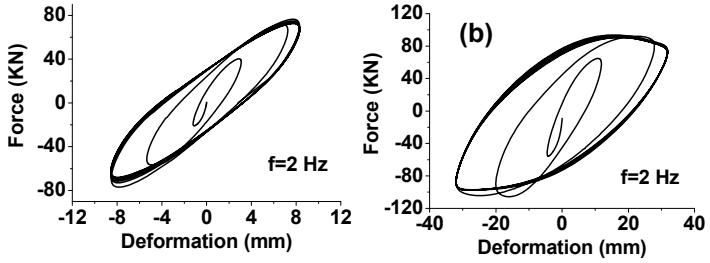

Figure 3. Typical hysteresis of prototype compressed elastomer dampers

The equivalent stiffness, K_{eq}, and the loss factor, η_{eq}, are often used to define the mechanical properties of damping materials. The K_{eq} is the ratio of the maximum force to the maximum displacement. The equivalent loss factor, η_{eq}, which represents the energy dissipation capacity (and is equivalent to η = G"/G' for a viscoelastic material), is determined as follows:

$$\eta_{eq} = \frac{ED}{2 \cdot \pi \cdot ES} \tag{1}$$

where *ED* is the energy dissipated per cycle of sinusoidal loading and *ES* is the maximum strain energy stored during a cycle of sinusoidal loading. K_{eq} and η_{eq} were determined from the characterization tests and are given in Fig 4. K_{eq} is for a pair of prototype dampers.

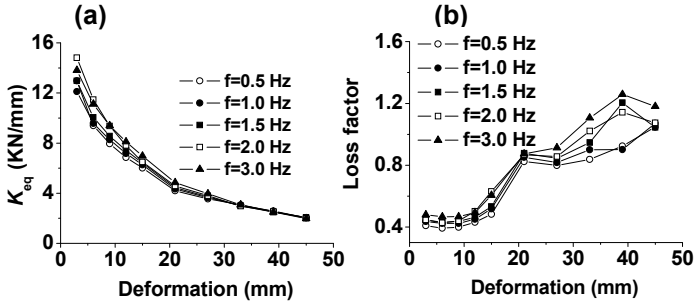

Figure 4. Mechanical properties evaluated from characterization tests: (a) equivalent stiffness, and (b) equivalent loss factor

Fig. 4(a)) shows that the stiffness (K_{eq}) decreases with increasing deformation amplitude, and slightly increases as the frequency increases, with the latter effect disappearing as the deformation increases. Fig. 4(b) shows that the energy dissipation (η_{eq}) is relatively constant for small amplitudes of deformation, significantly increases after slip of the elastomer initiates (relative to the tube) and slightly increases as the frequency increases.

Hysteretic Model for Dampers

Previous models for elastomeric dampers [e.g., Sause et al. 2007] are unable to simulate the combination of amplitude-dependent viscoelastic behaviour with post-slip friction behavior of the prototype compressed elastomer dampers. The proposed model for the hysteretic behavior of the prototype dampers consists of a parallel combination of a modified Bouc-Wen element [Wen 1976] with softening behavior, and a nonlinear dashpot, as shown in Fig. 5. The force output of the nonlinear dashpot is:

$$f_D = C \cdot |v|^{\alpha} \cdot \mathrm{sgn}(v) \tag{2}$$

where C is the damping coefficient, v is the deformation rate (relative velocity), α is a velocity exponent, and sgn is the signum function that provides the correct sign for the damping force. The force output of the Bouc-Wen element is:

$$f_{BW} = k \cdot p \cdot u + k \cdot u_y \cdot (1-p) \cdot z \tag{3}$$

where u_y is the yield (slip) displacement, p is the ratio of post-yielding to initial elastic stiffness, k, and z are dimensionless parameters governed by the following equation

$$\dot{z} = \frac{v}{u_y} \cdot \left[A - |z|^n \cdot (\beta \cdot \mathrm{sgn}(v \cdot z) + \gamma) \right] \tag{4}$$

where A, β and γ are constants that control the shape of the hysteresis loops, and n controls the rate of transition from the elastic to the yield state. To simulate the amplitude-dependent behavior (softening) of the damper before slip, the stiffness k of the Bouc-Wen model is modified as follows:

$$k = k_1 \cdot e^{-\frac{u_{max}}{u_{ref}}} + k_2 \tag{5}$$

where k_1, k_2 and u_{ref} are constants, and u_{max} is the average of the maximum absolute deformation amplitudes in negative ($u_{max,n}$) and positive ($u_{max,p}$) directions, as follows:

$$u_{max} = \frac{|u_{max,n}| + u_{max,p}}{2} \tag{6}$$

It is emphasized that $u_{max,n}$ and $u_{max,p}$ are used to distinguish between deformations in different directions. At each deformation increment the stiffness of the Bouc-Wen model is updated according to Eq. (5) by first updating the variable u_{max} using Eq. (6), while Eq. (4) is numerically integrated by using a Newton-Raphson scheme.

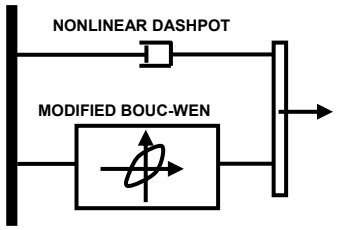

Figure 5. Proposed model for compressed elastomer damper

An unconstrained nonlinear minimization method was used to minimize the root mean square error between the measured force in the tests and the force from the model. Table 2 provides the parameters of the hysteretic model, while Fig. 6 shows that the characterization test data and results from the hysteretic model are in acceptable agreement.

Table 2. Damper model parameters determined from characterization tests

C kN/(mm/s.)^2	k_1 kN/mm	k_2 kN/mm	u_{ref} mm	u_y mm	a	p	A	n	β	γ
2.35	4.85	7.62	8.82	10	0.35	0.07	1.0	1.0	0.5	0.5

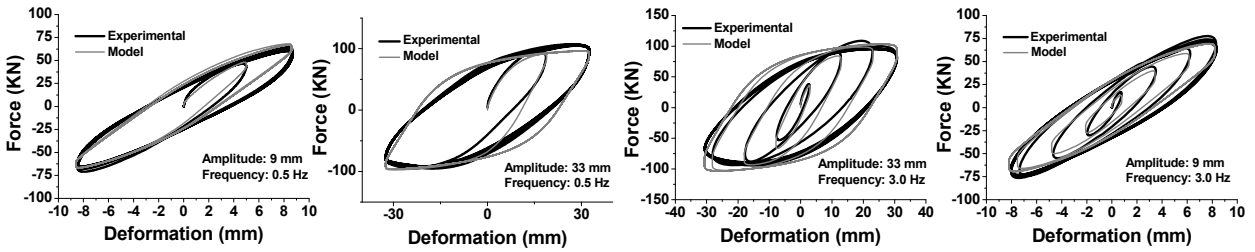

Figure 6. Comparison of experimental hysteresis and hysteretic model

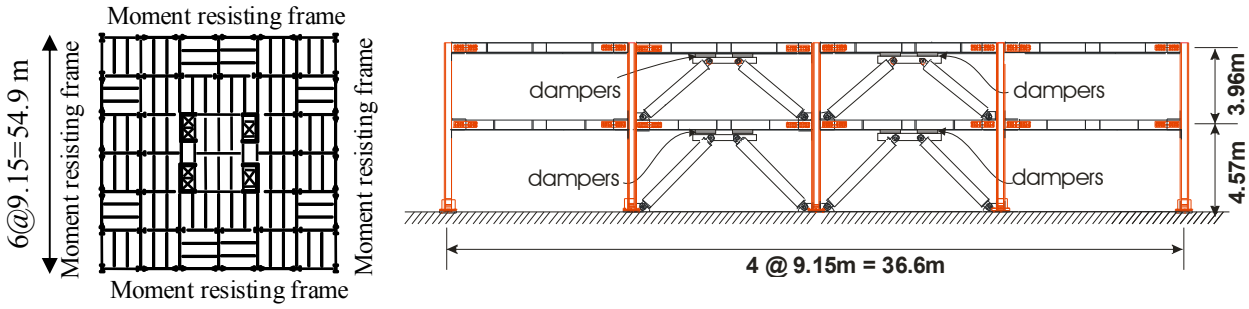

Figure 7. Prototype building structure: (a) plan view, and (b) perimeter MRF with dampers and supporting bracing

Steel MRFs with Compressed Elastomer Dampers

Prototype Building

Fig. 7(a) shows the plan view of the 2-story, 6-bay by 6-bay prototype office building used for the present study. The study focuses on one typical perimeter MRF. This MRF is designed either as a conventional special moment resisting frame (SMRF) as defined in the 2000

International Building Code (ICC 2000), referred to herein as IBC 2000, or as an MRF equipped with compressed elastomer dampers (Fig. 7(b)). The dampers are based on the prototype dampers that were tested, but the thickness and the area of the elastomer of the dampers were varied in the damper design process. The yield stress of the steel members of the MRF is 345 MPa. The gravity loads considered in the design are those described in IBC 2000. A smooth design response spectrum with parameters S_{DS}=1.0, S_{D1}=0.6, T_0=0.12 sec and T_s=0.6 sec (ICC 2000) represents the design basis earthquake (DBE).

Design of Perimeter MRF as a Conventional SMRF Without Dampers

The perimeter MRF in Fig. 7(b) is initially designed as a conventional SMRF using the equivalent lateral force procedure from IBC 2000. This SMRF without dampers, referred to herein as UD100V, satisfies the member strength criteria of IBC 2000 with a response modification factor, R, equal to 8 and also the 2% story drift limit of IBC 2000 with a displacement amplification factor, C_d, equal to 5.5. Different versions of the perimeter MRF were designed without dampers to have design base shears equal to $0.75V$, $0.50V$ and $0.25V$, where V is the design base shear of UD100V. The resulting MRF options, referred to herein as UD75V, UD50V and UD25V, do not satisfy the drift criteria of IBC 2000. Table 3 provides properties of the four MRF design options (UD100-75-50-25V). The table lists column and beam sections, elastic fundamental period of vibration (T_1), and the maximum story drift, θ_{max}, under the DBE earthquake. The maximum story drift, θ_{max}, is estimated on the basis of the equal displacement rule.

Table 3. Properties of MRF designs

MRF Design	Column Section	Beam Section	Steel Weight (kN)	T_1 (sec)	θ_{max} (%)
UD100V	W14x211	1st story: W24x84 2nd story: W21x50	200	1.08	2.40
UD75V	W14x159	1st story: W24x68 2nd story: W21x44	156	1.26	2.80
UD50V	W14x120	1st story: W24x55 2nd story: W18x40	124	1.48	3.23
UD25V	W14x90	1st story: W21x44 2nd story: W16x31	95	1.83	4.00

Design of Dampers for MRFs

Various damper designs were generated for the four MRF design options. The damper designs are based on the prototype compressed elastomer damper described earlier, but the thickness, t, and area, A, of the dampers are varied from those of the prototype damper.

The properties of the compressed elastomer damper designs were derived from the experimental data presented in Fig. 4 as follows. With t_{ref} and A_{ref} as the thickness and area, respectively, of the elastomer in the prototype damper assembly that was tested, the properties of the damper designs are expressed in terms of the ratios t/t_{ref} and A/A_{ref}. Given the stiffness, $K_{eq}(u_{ref})$, and the loss factor, $\eta_{eq}(u_{ref})$, of the prototype damper assembly that was tested, the

stiffness and loss factor of the damper designs are $K_d(u_d) = (A/A_{ref})(t_{ref}/t)K_{eq}(u_{ref})$ and $\eta_d(u_d) = \eta_{eq}(u_{ref})$, where u_d is the deformation imposed on the damper in the MRF, and u_{ref} is the deformation of the prototype damper assembly that was tested, related to u_d through the expression $u_{ref}=u_d\cdot(t_{ref}/t)$. These expressions are derived by transforming the test results for the prototype damper assembly from force-deformation (F_{ref}-u_{ref}) behavior to shear stress-shear strain (τ-γ) behavior using the t_{ref} and A_{ref} dimensions (i.e., $\tau=F_{ref}/A_{ref}$ and $\gamma=u_{ref}/t_{ref}$) and transforming the shear stress-shear strain (τ-γ) behavior to force-deformation (F_d-u_d) behavior of the damper designs using t and A (i.e, $F_d=F_{ref}\cdot A/A_{ref}$ and $u_d=u_{ref}\cdot t/t_{ref}$). For all of the damper designs A/A_{ref} was equal to 4, which provides a practical full-scale damper size. The damper designs used different values of t/t_{ref} and a different numbers of dampers.

The simplified design procedure (SDP) developed by Lee *et al.* (2005) was modified and employed to design the dampers for the MRF options. The damper design variables are the equivalent damper stiffness, $K_d(u_d)=(A/A_{ref})\cdot(t_{ref}/t)\cdot K_{eq}(u_{ref})$, and the loss factor, $\eta_d(u_d)= \eta_{eq}(u_{ref})$. For a given MRF and performance criteria, the following iterative design procedure is employed:
(1) *Select an appropriate α value (ratio of total brace stiffness per story in the global direction to the MRF story stiffness).* This ratio should provide: (a) braces that are stiff enough so that the story drift produces damper deformation with minimal brace deformation; and (b) braces which do not buckle under the maximum forces transmitted by the dampers
(2) *Select an appropriate β value (ratio of total damper stiffness per story in the global direction to the MRF story stiffness).* The β value should provide a reasonable required number of dampers.
(3) *Select an initial value of the damper loss factor, η_d.* With the η_d known, the contribution of the dampers to the damping ratio of the MRF with the dampers, ξ_{eq}, is estimated based on the lateral force energy method (Sause et al. 1994). Then, the damping reduction factor, B, can be easily obtained (BSSC 2001) as a function of the total damping ratio for the MRF building with dampers, ξ_t, which equals ξ_{eq} plus the inherent damping ratio of the building (assumed to be 2%).
(4) *Response spectrum analysis.* The elastic response spectrum is reduced by the B factor, and story drifts and damper deformation, u_d, are estimated using the equal-displacement rule. The $\eta_d(u_d)= \eta_{eq}(u_{ref})$ is calculated from the damper characterization test data for the prototype damper shown in Fig. 4(b) using $u_{ref}=u_d\cdot(t_{ref}/t)$. Iterations of steps 3 and 4 are performed until the loss factor converges. If story drifts after convergence do not satisfy the performance criteria, steps 2 to 4 are repeated, beginning by selecting a new value of β. If a satisfactory value for β cannot be established, then the performance criteria and/or a new MRF should be considered and steps 1 to 4 repeated.
(5) *Calculate required number of dampers*. The damper design stiffness is determined from the damper characterization test data shown in Fig. 4(a) as follows: $K_d(u_d) = (A/A_{ref})(t_{ref}/t)K_{eq}(u_{ref})$. The required number of dampers, N_d, equals ($\beta/K_d(u_d)$) times the story stiffness, rounded up to the nearest integer.

Table 4 provides a summary of the damper design based on the UD50V MRF design. t/t_{ref} was assigned values of 2.0, 3.0 and 4.0 in order to identify the influence of t/t_{ref} on the resulting designs and the corresponding estimated drift and deformation demands. Table 4 provides the estimated story drift, θ_{max}, the ratio of the damper deformation, u_d, to the damper slip deformation, $u_{d.slip}$, the ratio of the damper deformation, u_d, to the damper damage deformation, $u_{d.dam}$, and the required number of dampers, N_d. Based on the characterization tests described previously in this paper, $u_{d.slip}$ is assumed approximately equal to (t/t_{ref})15 mm, while $u_{d.dam}$ is assumed approximately equal to (t/t_{ref})45 mm. Different values of α and β are considered to obtain frame designs with a performance level similar to (θ_{max} close to 2.0% for α=5 and β=0.5) and better than (θ_{max} close to 1.5% for α=10 and β=1.0) the performance of the conventional SMRF.

Table 4. Design of UD50V with dampers varying the value of t/t_{ref}

t/t_{ref}	α	Brace weight (kN)	β	ξ_t (%)	B	θ_{max} (%)	$u_d/u_{d.slip}$	$u_d/u_{d.dam}$	N_d Story 1st	N_d Story 2nd
2	5	8.6	0.5	14.6	1.35	1.90	2.68	0.84	5	3
3	5	8.6	0.5	13.3	1.30	2.00	1.83	0.58	5	3
4	5	8.6	0.5	12.6	1.28	2.03	1.37	0.44	5	3
2	10	17.2	1.0	20.0	1.50	1.53	2.11	0.66	8	6
3	10	17.2	1.0	19.0	1.47	1.56	1.40	0.45	8	6
4	10	17.2	1.0	15.0	1.35	1.65	1.14	0.37	8	5

Table 5. Design of various MRF options with dampers for t/t_{ref}=4

Design	Frame	α	Brace weight (kN)	β	T_1 (sec)	ξ_t (%)	B	θ_{max} (%)	N_d Story 1st	N_d Story 2nd
D1	UD25V	12.5	15.2	1.0	1.24	18.0	1.44	1.90	6	4
D2	UD25V	20.0	24.3	2.0	1.03	20.0	1.50	1.55	10	6
D3	UD50V	5.0	8.6	0.5	1.18	12.6	1.28	2.03	5	3
D4	UD50V	10.0	17.2	1.0	1.04	15.0	1.35	1.65	8	5
D5	UD75V	5.0	11.7	0.5	1.02	11.0	1.24	1.85	6	4
D6	UD75V	10.0	23.4	1.0	0.88	13.0	1.29	1.50	9	6
D7	UD100V	5.0	15.7	0.5	0.88	9.8	1.20	1.60	7	4

For the case of a thickness ratio of t/t_{ref} = 4.0 in Table 4, the following observations are made: (a) the damper deformation is slightly larger than $u_{d.slip}$ which means that slip in the dampers may occur in the DBE; and (b) a large margin of damper deformation relative to $u_{d.dam}$ is provided so that the dampers should not be heavily damaged under earthquakes larger than the DBE. For the various cases of t/t_{ref} in Table 4, the following observations are made: (c) the required number of dampers is not influenced by t/t_{ref}; (d) MRFs with dampers with higher performance than that of the UD100V can be obtained even when they are significantly lighter in than the UD100V; (e) the required number of dampers is practical; and (f) a significant reduction in the MRF steel weight can be obtained by using compressed elastomer dampers. Note that the steel weight of the conventional UD100V SMRF is 200 kN (Table 3), while the steel weight of the UD50V MRFs with dampers in Table 4 is equal to 124 kN (UD50V) + 8.6 kN (weight of braces) = 132.6 kN and 124 kN (UD50V) + 17.20 kN (weight of braces)= 141.2 kN for values of α equal to 5 and 10, respectively.

Table 5 provides information for various MRFs with dampers (D1 through D7) designed with t/t_{ref} equal to 4. The story drift and damper deformation demand estimates are for the DBE. The observations for Table 4 are seen again for Table 5. In addition, it is seen that the dampers and bracing system are more effective for lighter, more flexible frames.

Nonlinear Time History Analyses

An ensemble of 25 earthquake ground motions recorded on stiff soil sites (without near-fault effects) were used in nonlinear dynamic time history analyses (NDTHA) to evaluate the performance of the conventional SMRF UD100V and the performance of the MRFs with compressed elastomer dampers given in Table 5. The ground motions were scaled to the DBE level using the scaling procedure of Somerville (1997). The amplitudes of the DBE ground motions were further scaled by 1.5 to represent MCE ground motions. The NDTHA were performed using OpenSEES (Mazzoni et al. 2006). The hysteretic constitutive model for the compressed elastomer damper described earlier was implemented into OpenSEES and used to model the dampers. Fig. 8 compares the θ_{max} for the various MRF designs with dampers with the maximum story drift obtained from the NDTHA. It is observed that the median θ_{max} values for the DBE are consistent with the θ_{max} design demand used in the SDP to design the MRFs with dampers (Table 5). Under the MCE, the frames with dampers show better performance than the conventional SMRF (UD100V) which has a median θ_{max} of 3.25%.

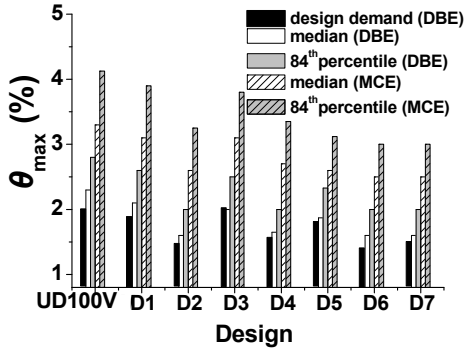

Figure 8. Comparison of median and 84th percentile values of maximum story drift under DBE and MCE

Table 6. Median values of response parameters under the DBE

Design	Beam plastic rotation (rad)	Column plastic rotation (rad)	Floor velocity (m/s.)	Floor acceleration (m/s.^{2})
UD100V	0.006	0.007	0.96	5.40
D1	0.002	0.003	0.87	4.70
D2	0.001	0.001	0.97	5.72
D3	0.005	0.003	0.97	4.70
D4	0.003	0.002	0.97	5.70
D5	0.002	0.005	1.00	5.80
D6	0.001	0.002	1.00	6.70
D7	0.002	0.002	1.00	6.70

Table 6 presents statistics for the peak beam and column plastic rotations obtained from the NDTHA under the DBE ground motions for the various designs. The MRFs with dampers show significant decreases in plastic rotations. Table 6 also presents the peak floor velocity and peak floor acceleration response of the various designs obtained from the NDTHA. In general, the MRFs with dampers have peak floor velocities and peak floor accelerations similar to those of

the UD100V SMRF. Designs D6 and D7 have noticeably larger peak floor accelerations because they have a shorter fundamental period of vibration T_1 and a low total damping ratio ξ_t.

Summary and Conclusions

Based on the results of nonlinear seismic response analyses of MRFs with dampers the following conclusions were drawn: (1) MRFs with compressed elastomer dampers can be designed to perform better than conventional SMRFs, even when the MRF with dampers is significantly lighter in weight than the conventional SMRF; (2) the damper becomes more effective for lighter steel MRFs; (3) the dampers are effective in reducing story drifts and plastic hinge rotations in the steel MRFs; and (4) the combination of compressed elastomer dampers with light flexible steel MRFs can lead to a satisfactory control of drift and floor acceleration.

Acknowledgements

This paper is based upon work supported by grants from the Pennsylvania Department of Community and Economic Development through the Pennsylvania Infrastructure Technology Alliance, and by the National Science Foundation (NSF) under Grant No. CMS-04002490 within the George E. Brown, Jr. Network for Earthquake Engineering Simulation Consortium Operation. The elastomeric dampers were manufactured and donated to the research project by Corry Rubber. Any opinions, findings, and conclusions expressed in this paper are those of the authors and do not necessarily reflect the views of the sponsors.

References

Building Seismic Safety Council (BSSC) 2001. NEHRP recommended provisions for seismic regulations for new buildings and other structures, 2000 Ed., Report FEMA 368, Federal Emergency Management Agency, Washington, D.C.

International Code Council (ICC) 2000. *International Building Code*, Falls Church, VA.

Karavasilis TL, Sause R, Ricles JM. 2009. Seismic design and evaluation of steel MRFs with compressed elastomer dampers. *Earthquake Engineering and Structural Dynamics*, under review.

Lee KS, Fan CP, Sause R, Ricles J. 2005. Simplified design procedure for frame buildings with viscoelastic or elastomeric structural dampers. *Earthquake Engineering and Structural Dynamics* 34:1271-1284.

Mazzoni S, McKenna F, Scott M, Fenves G. 2006. Open System for Earthquake Engineering Simulation (OpenSees). User Command Language Manual, Version 1.7.3, Pacific Earthquake Engineering Research Center, University of California, Berkeley.

Sause R, Lee KS, Ricles J. 2007. Rate-independent and rate-dependent models for hysteretic behavior of elastomers. *Journal of Engineering Mechanics* 133(11):1162-1170.

Sause R, Hemingway GJ, Kasai K. 1994. Simplified seismic response analysis of viscoelastic-damped frame structures. *Proceedings, 5th U.S. National Conference on Earthquake Engineering*, EERI, Chicago, Illinois, Vol. I, 839-848.

Somerville P. 1997. Development of ground motion time histories for Phase 2 of the FEMA/SAC Steel Project, Report No. SAC/DB-97/04, Sacramento, CA.

Sweeney SK, Michael R. 2006. Collaborative product realization of an innovative structural damper and application. *Proceedings of IMECE2006, ASME International Engineering Congress and Exposition*, Chicago, Illinois, USA.

Wen YK. 1976. Method for random vibration of hysteretic systems. *Journal of Engineering Mechanics Division* 102(2):249-263.